RESEARCH ARTICLE

Experimental investigation on hydrate dissociation in near-wellbore region caused by invasion of drilling fluid: ultrasonic measurement and analysis

Qingchao Li[1,2,3] · Yuanfang Cheng[2] · Ubedullah Ansari[4] · Ying Han[1] · Xiao Liu[1] · Chuanliang Yan[2]

Abstract

As we all know, development and utilization of clean energy is the only way for society to achieve its sustainable development. Although natural gas hydrates is a new type of clean energy, uncontrollable hydrate dissociation and accompanying methane leakage in drilling operation threaten drilling safety, as well as marine environment. However, the dissociation range of natural gas hydrates around wellbore cannot be reasonably determined in previous investigations, which may lead to the inaccurate estimation of borehole collapse and methane leakage. Then, the marine environment will be greatly damaged or affected. The purpose of the present work is to experimentally explore the dissociation characteristics of gas hydrates around wellbore in drilling operation and analyze the influence law and mechanism of various factors (such as hydrate saturation) on hydrate dissociation. It is expected to provide reference for exploring effective engineering measures to avoid the uncontrolled hydrate dissociation, borehole collapse and accompanying methane leakage. The experimental results demonstrate that acoustic velocity of hydrate-bearing sediment can be accurately expressed as quadratic polynomial of hydrate saturation, which is the theoretical basis for determination of hydrate saturation in subsequent experiments. Owing to the fact that hydrate dissociation is an endothermic reaction, hydrate dissociation gradually slows down in experiment. Throughout the experiment, the maximum dissociation rate at the beginning of the experiment is 8.69 times that at the end of the experiment. In addition, sensitivity analysis found that the increase in the stabilizer concentration in drilling fluid can inhibit hydrate dissociation more effectively than the increase in the hydrate saturation. Hydrate dissociation was completely inhibited when the concentration of soybean lecithin exceeds 0.60wt%, but hydrate dissociation definitely occurs in the near-wellbore region no matter what hydrate saturation is. In this way, based on the requirements of drilling safety and/or environment protection, hydrate dissociation and accompanying methane leakage can be controlled by designing and adjusting the stabilizer concentration in drilling fluid.

Keywords Hydrate-bearing sediments · Hydrate dissociation · Drilling fluid invasion · Methane leakage · Marine environment · Ultrasonic measurement

✉ Qingchao Li
liqingchao2020@hpu.edu.cn

Yuanfang Cheng
yfcheng@upc.edu.cn

1 School of Energy Science and Engineering, Henan Polytechnic University, Jiaozuo 454000, China

2 School of Petroleum Engineering, China University of Petroleum (East China), Qingdao 266580, China

3 Key Laboratory of Unconventional Oil & Gas Development, Ministry of Education, (China University of Petroleum (East China)), Qingdao 266580, P. R. China

4 Institute of Petroleum & Natural Gas Engineering, Mehran University of Engineering and Technology, Jamshoro 76062, Pakistan

Introduction

Oil and gas are still the main energy to promote social development and ensure people's normal life. However, utilization of the traditional energy pollutes the environment, and it is also a non-renewable resource (Yang et al. 2020; Zhong et al. 2020; Yao et al., 2022). Therefore, exploring new energy is the key to realize sustainable development of society. Natural gas hydrates are ice-like cage crystals composed of host water molecules and guest natural gas molecules (methane commonly consists more than 95%) under low-temperature and high-pressure conditions (Sloan 2003; Ye et al. 2018; Liu et al. 2021). In nature, gas hydrates are mainly buried in offshore sediments, and also diffused in a small amount in permafrost, the total global reserves amount to 2.1×10^{16} m^3 (Zhang et al. 2021; Gambelli 2021). In addition to huge reserves, utilization of gas hydrates is environmentally friendly, and

the combustion products are almost only carbon dioxide (CO_2) and water (H_2O) (Misyura 2020). Owing to the above-mentioned two aspects, natural gas hydrates have been attracting significant global attention, and a series of offshore trial production activities have been performed in recent years (Zhu et al. 2021; Sahu et al., 2021). Among them, China's second production test in the South China Sea in 2020 achieved a satisfactory result of producing 8.614×10^5 m^3 of methane within one month (Ye et al. 2020; Zhu et al. 2021; Sahu et al., 2021). It is believed that with the gradual improvement of exploitation techniques, natural gas hydrates are likely to become a potential alternative energy source for oil and gas in the near future (Zhao et al. 2019b; Wang et al. 2021b).

Nevertheless, some issues will probably occur during drilling or exploitation of natural gas hydrates offshore (Yan et al. 2018, 2020; Song et al. 2019; Yang et al. 2021; Li et al. 2021a). Among them, as presented in Fig. 1, hydrate dissociation around wellbore and borehole collapse caused

Fig. 1 Hydrate dissociation around wellbore and borehole collapse while drilling in hydrate reservoir
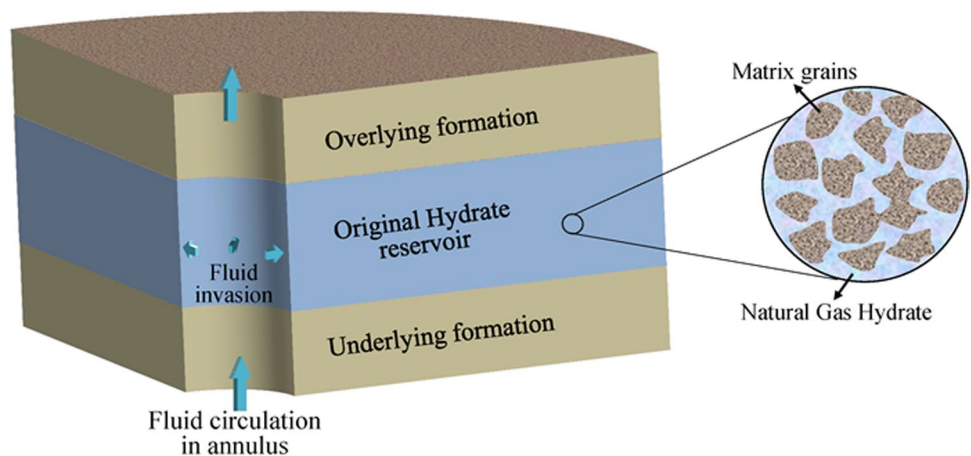
(a) Initial state of borehole and hydrate reservoir
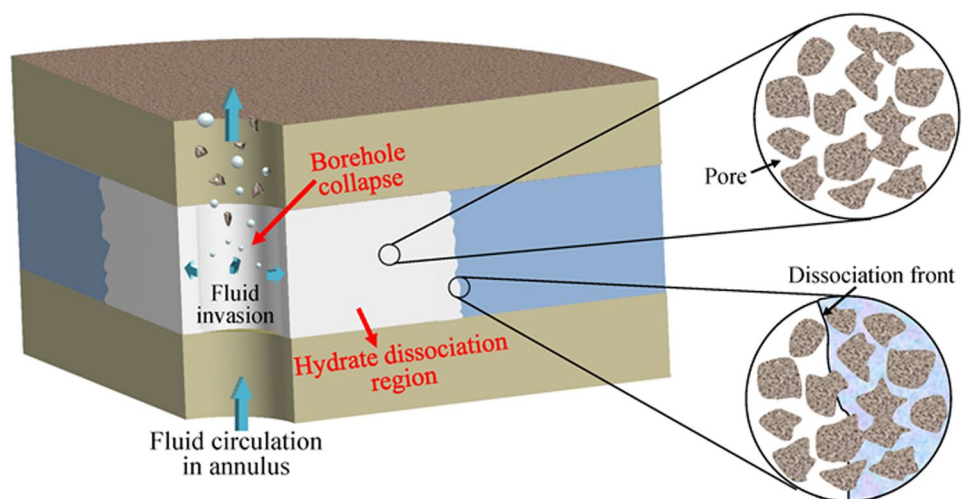
(b) Hydrate dissociation and borehole collapse caused by fluid disturbance

by drilling fluid disturbance during drilling operation is one issue that cannot be ignored (Li et al. 2020). As shown in Fig. 1a, natural gas hydrates in the near-wellbore region are stable before or at the beginning of drilling operation, almost no hydrates dissociate (Li et al. 2021b). At this time, borehole stability can be well maintained because natural gas hydrates have not yet begun to dissociate and the sediment strength is high (Li et al. 2021a). However, the borehole directly or indirectly contacts with drilling fluid while drilling in hydrate reservoir, and invasion of drilling fluid into hydrate reservoir is inevitable (Salehabadi 2009). Generally speaking, disturbance of drilling fluid on reservoir temperature and reservoir pressure persists throughout the drilling operation (Golmohammadi and Nakhaee 2015). As demonstrated in Fig. 1b, changes in sediment temperature and sediment pressure in the near-wellbore region will cause hydrate dissociation (Song et al. 2019), reduction in the sediment strength (Yan et al. 2017; Cheng et al 2021; Yao et al., 2021) and borehole instability (Li et al. 2020). Borehole collapse will significantly affect the subsequent cementing operation, and the cementing quality will decline to a certain extent. In this case, the integrity of wellbore is extremely difficult to guarantee during methane production from gas hydrates (Salehabadi 2009). What is more, borehole collapse will also prolong the drilling cycle and increase the drilling costs (Ashena et al. 2020; Zhao et al. 2019a). The gas produced in offshore drilling operation is usually directly discharged into the atmosphere. So, methane leakage caused by uncontrollable hydrate dissociation is also an important environmental issue during drilling operation in hydrate reservoir. Fortunately, adding appropriate concentrations of stabilizers (such as lecithin) to the drilling fluid can alleviate this situation to a certain extent (Zhao et al. 2019b; Wang et al. 2021a). Therefore, it is of great importance to perform experimental and theoretical studies on stability of gas hydrates around wellbore for safe and efficient drilling operation in hydrate reservoir, as well as protection of marine environment.

In recent years, several studies regarding the effect of drilling fluid on hydrate reservoir during drilling operation have been performed. All these studies are helpful to further explore the engineering measures to prevent excessive hydrate dissociation around wellbore and uncontrollable wellbore instability during drilling operation in hydrate-bearing sediments. To name a few, Huang et al. (2020) experimentally explored the disturbance of drilling fluid with different circulation rates on hydrate-bearing sediments in drilling operation and found that both the temperature increase region around wellbore and gas production increase with the increase in the circulation rate. Gao et al. (2019) measured the temperature change of hydrate-bearing sediments around wellbore in drilling operation, indicating that heat transfer in hydrate reservoir can be divided into six periods, which is complex than that in conventional reservoir.

Yu et al. (2018) investigated gas production from hydrates and gas kick during drilling through hydrate reservoir, and the results show that hydrate dissociation was significantly affected by factors such as drilling fluid temperature and pressure. Freij-Ayoub et al. (2007) inspected both hydrate dissociation and wellbore stability in hydrate reservoir by developing a coupling model and found that physical field was an important factor affecting hydrate dissociation in hydrate deposits. Ning et al. (2013a, b) numerically analyzed the effect of drilling fluid invasion on reservoir temperature, reservoir pressure and hydrate dissociation by using a 1D model. The simulation results show that the disturbance of drilling fluid invasion on hydrate stability is related not only to the drilling fluid properties, but also to reservoir characteristics.

To the best of the authors' knowledge, there are two shortcomings in previous investigations. For one thing, relevant experimental investigations mainly focus on the influence of drilling fluid disturbance on reservoir temperature and reservoir pressure in the near-wellbore region, rather than on hydrate dissociation. Even if there are some studies on hydrate dissociation around wellbore in drilling operation, hydrate dissociation is indirectly described by gas production, rather than directly by the distribution of hydrate saturation. In this way, the dissociation range of gas hydrates around wellbore in previous experimental studies is difficult to be accurately determined. Notably, borehole collapse is difficult to be reasonably evaluated if the dissociation range of gas hydrates around wellbore is not clear, because mechanical properties of hydrate deposits are directly related to hydrate saturation. For another, although some numerical investigations directly presented the distribution of hydrate saturation around wellbore in drilling operation, the simulation results are usually lack of credibility verification. In short, despite the fact that some progress has been made in current research, further exploration and improvement are still required. Most importantly, the formation and dissociation of gas hydrates in sediments are difficult to be observed through human eyes. Therefore, it is necessary to experimentally illustrate hydrate dissociation around wellbore while drilling in hydrate reservoir directly through hydrate saturation by certain technical means.

Inspired by the previous studies, an apparatus was designed for directly investigating hydrate dissociation around wellbore in drilling operation by measuring the distribution of hydrate saturation. First, the relationship between hydrate saturation in sediment and P-wave velocity was determined with experiments, which could serve as the basis for determining hydrate saturation according to P-wave velocity obtained in experiments. Then, evolution characteristics of hydrate dissociation around wellbore caused by drilling fluid disturbance during drilling operation in hydrate-bearing sediments were explored in detail.

Finally, in order to lay the foundation for putting forward practical engineering measures to avoid wellbore instability and uncontrollable methane leakage, factors (such as stabilizer concentration and hydrate saturation) affecting hydrate dissociation around wellbore were investigated. This work provides basic experimental data for numerical prediction of both borehole collapse and methane leakage in hydrate reservoir offshore, as well as verification of the relevant multi-field coupled simulation model.

Experimental section

Materials

Methane (CH4, 99.99% purity) supplied by Zhengzhou Xingdao Chemical Technology Co., Ltd. was used for hydrate preparation in this study. The low-viscosity poly-anionic cellulose (PAC-LV), amphoteric polymer (FA-367) and sulfonated phenolic resin (SMP), as additives of water-based drilling fluid, were all provided by Sinopec Offshore Oil Engineering Co., Ltd. The soybean lecithin was donated by Nanjing Ruize Fine Chemical Co., Ltd, and it was used as hydrate stabilizer. Marine soil used for preparation of hydrate-bearing sediment was obtained in Shenhu area of the South China Sea and was provided by the Institute of Deep-sea Science and Engineering, CAS.

We all know that soil samples obtained from hydrate reservoir offshore through drilling operation are limited and precious. Artificial preparation of sediment according to the composition and particle size distribution is a feasible method for subsequent studies on hydrate-bearing sediment. The particle size distribution results of hydrate-bearing sediment provided by the Institute of Deep-sea Science and Engineering, CAS, are given in Table 1. As observed in Table 1, sediment minerals are mainly composed of clay and fine silt (more than 50%).

Experimental apparatus

Figure 2 illustrates the piping and instrumentation diagram of the experimental apparatus used in this study. Both in situ preparation of hydrate-bearing sediments and hydrate

Table 1 Particle size distribution results of hydrate-bearing sediment

Minerals	Percentage, %
Clay ($<3.9um$)	23.5
Fine silt ($3.9 \sim 15.6um$)	34.3
Coarse silt ($15.6 \sim 63.0um$)	35.2
Fine sand ($63.0 \sim 250.0um$)	4.8
Sand (>250.0 mm)	2.2

dissociation experiments can be conducted with this apparatus. The apparatus mainly consists of a hydrate in situ formation and dissociation unit, a fluid circulating unit, a pressure controlling unit and an ultrasonic measurement system. The autoclave (radius: 31 cm, height: 6 cm, wall thickness: 1 cm, material: 316L stainless steel) filled with sediments needs to be placed in cold storage (refrigeration limit: -50 degrees Celsius) throughout the experiment, and its inlet is connected to a methane cylinder by needle valve 2. During preparation of hydrate-bearing sediments, sufficient methane can be continuously supplied to the sediment in autoclave by the methane cylinder (volume: 40L). A gas–liquid separator is connected with the outlet of autoclave, and the dissociation gas can be effectively separated and measured from the gas–liquid mixture in circulating pipeline. The circulating pump (maximum flow: 5.0L/min, weight: 5.2 kg) connected with the separator can realize constant-flow circulation of drilling fluid in apparatus, and the flow rate in all experiments is 2.0L/min. The temperature control tank (volume: 20L) can heat and insulate the drilling fluid circulated in apparatus, and the heating limit is 100 degrees Celsius. The pressure control unit is composed of two servo pumps (precision: 0.05L/min), which can be used for controlling the bottom-hole pressure and the reservoir pressure, respectively.

The ultrasonic measurement system (frequency range: 0.01–1.00 MHz) is the apparatus core, and it is purchased from Yangzhou Oriental Ultrasound Technology Co., Ltd. Figure 3 shows the schematic of measurement principle of ultrasonic measurement system. As highlighted in Fig. 3a and b, 40 sets of transducers are evenly arranged on the upper and lower surfaces of the autoclave in five radial paths. The distance between two adjacent transducers in one radial path is 3.0 cm. As shown in Fig. 3c and d, in experiment, the ultrasonic is excited by the transmitting transducer and received by the receiving transducer after being attenuated by sediment. Then, the received acoustic wave velocity was automatically transmitted back to the acoustic measurement system for data processing.

Experimental method

The whole experiment roughly covered two steps: preparation of hydrate-bearing sediment and hydrate dissociation experiment. The research framework (i.e., logical structure) is presented in Fig. 4, and the detailed description of experimental method is given in this section.

Preparation of hydrate-bearing sediments

The reaction of methane and water to form methane hydrate at low temperature and/or high pressure can be expressed as (Joseph et al. 2017):
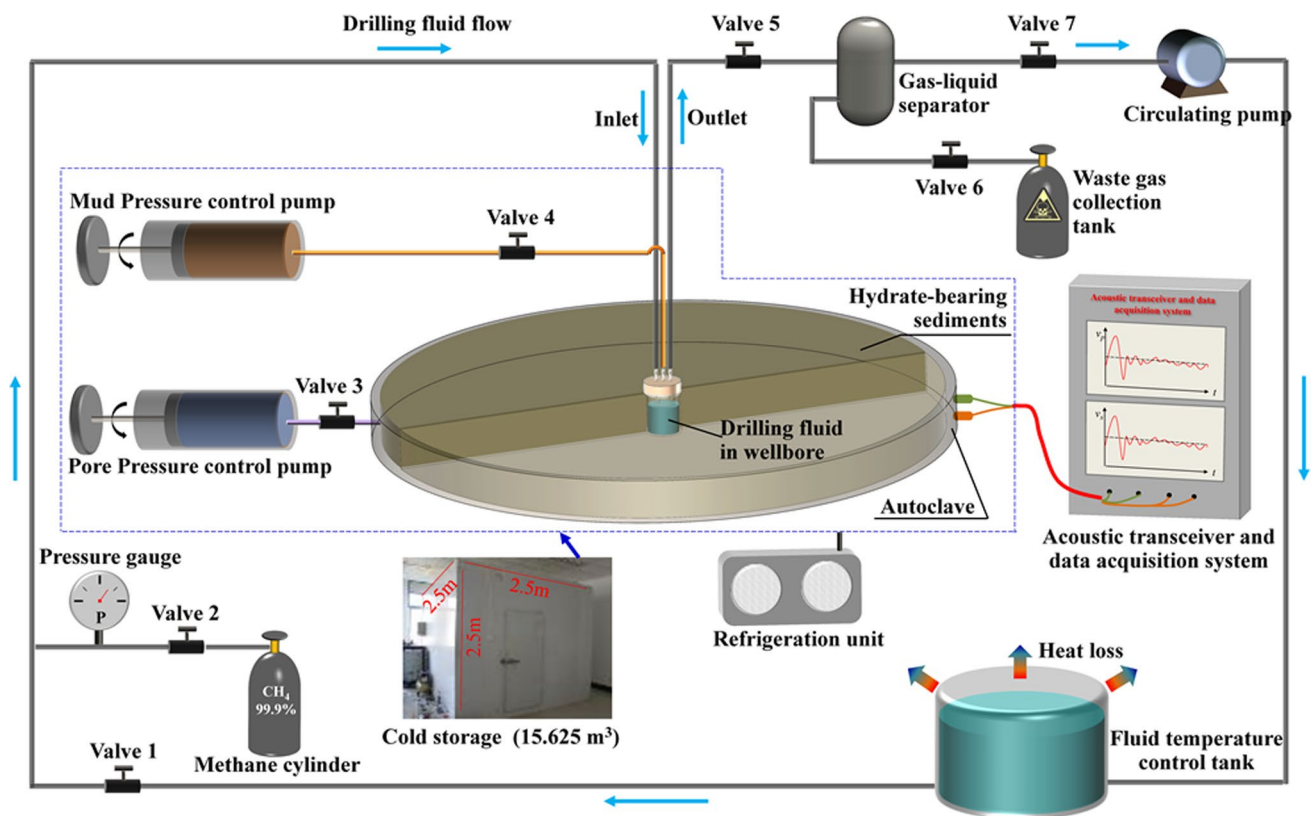
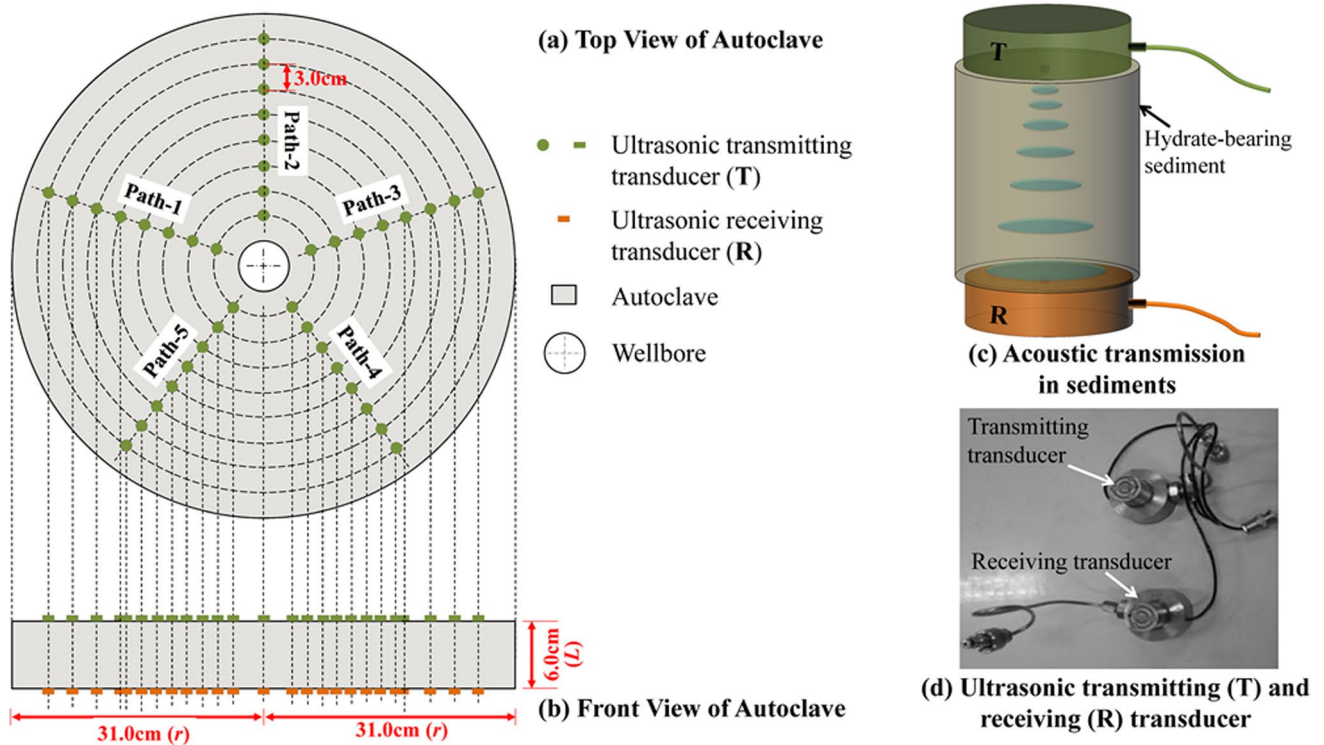**Fig. 2** Piping and instrumentation diagram of the experimental system used in this paper

Fig. 3 Installation and measurement principle of ultrasonic receiving transducer (R) and transmitting transducer (T)
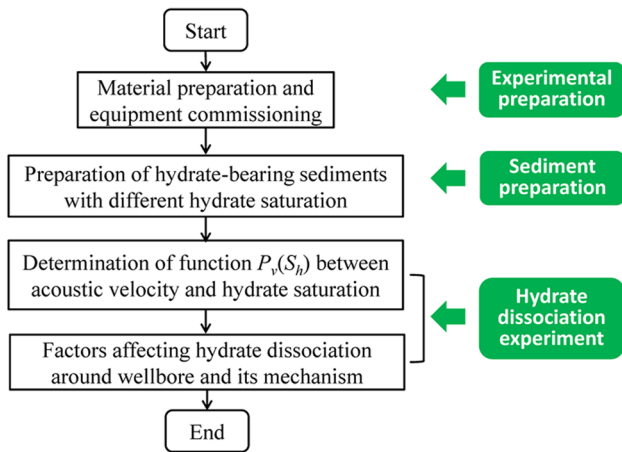
Fig. 4 Research framework in the present work

$$CH_4 + nH_2O \Leftrightarrow CH_4nH_2O \quad (Reaction1)$$

Hydrate-bearing sediments were prepared in laboratory by using the marine soil obtained in the study area, and Fig. 5 shows the preparation process. As displayed in Fig. 5, the "excess gas method" was used to prepare hydrate-bearing sediments in this study (Sell et al. 2016). During the preparation, the marine soil needs to be dried and crushed (particle structure should not be destroyed) first. Then, distilled water with mass of m_w is measured and fully mixed with the dry soil in autoclave. The mass of water m_w was determined by Eqs. (1):

$$m_w = \frac{207}{239}V\varphi S_\varphi \rho_h \quad (1)$$

where V is the internal volume of autoclave, φ is the porosity of hydrate-bearing sediment, S_h is the hydrate saturation and ρ_h is the hydrate density (0.91 g/cm^3).

After that, the mixture of water and soil in autoclave is compacted with a pressure of about 2.80 MPa. The purpose is to restore the compaction state of sediments in shallow environment at a depth of ~200 m below the seafloor. Finally, adjust the experimental temperature in cold storage below the phase equilibrium temperature, and continuously inject sufficient methane into autoclave until the autoclave pressure is constant. Preparation time of hydrate-bearing sediments may last for ~1 to 3 days, which depends on hydrate saturation. In this study, seven hydrate-bearing sediments with hydrate saturation of 0, 0.08, 0.16, 0.24, 0.32, 0.40 and 0.48 were prepared.

Microstructure is an important means for us to explore the distribution of gas hydrate in hydrate-bearing sediments, and the micrograph of hydrate-bearing sediments with hydrate saturation of 0.24 is shown in Fig. 6. As observed in Fig. 6, gas hydrates are filled in pores of hydrate-bearing sediment in the form of crystal particles. Although this distribution form of gas hydrates in hydrate-bearing sediments cannot cement the sand particles like argillaceous cement, it can also share the pressure borne by the pore fluid (water and gas). Actually, this is also one of the mechanisms by which gas hydrates enhance the anti-deformation ability of hydrate-bearing sediments. According to our conjecture, with the increase in the hydrate

Fig. 5 Preparation procedure of hydrate-bearing sediments
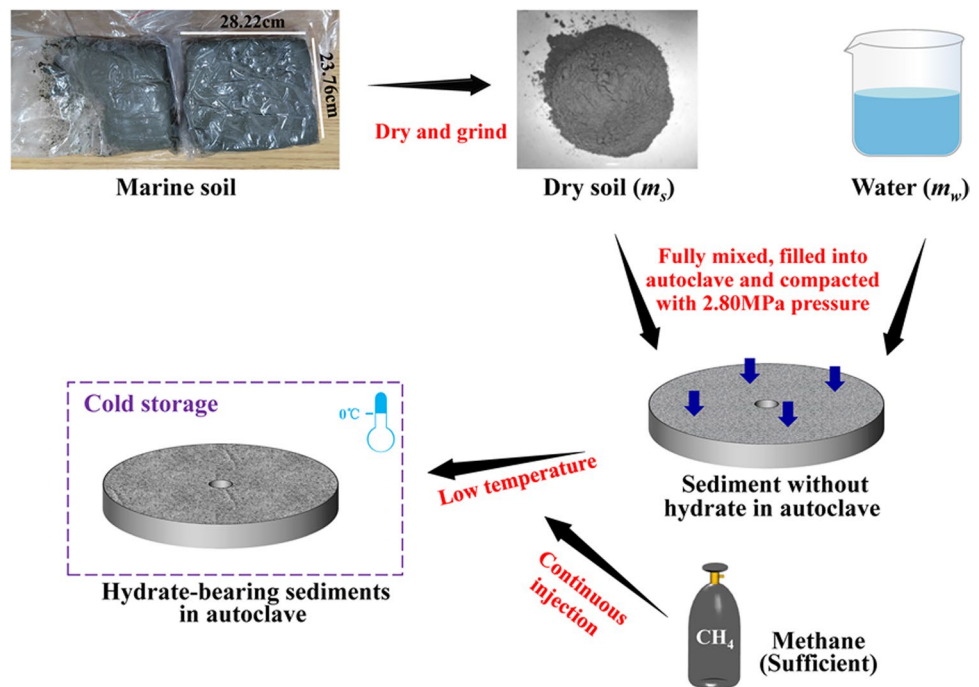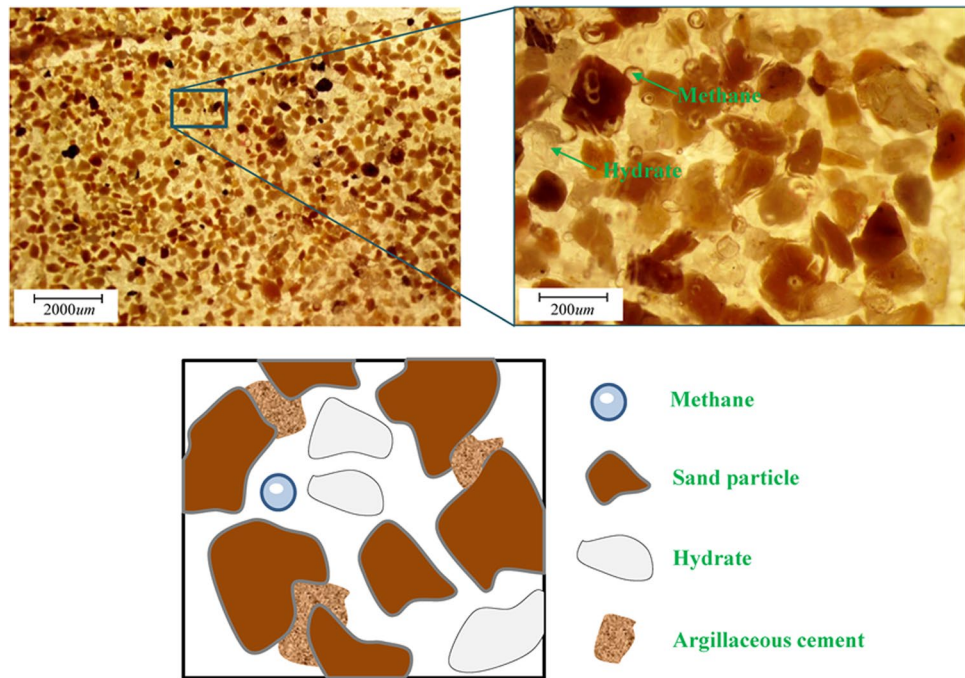
Fig. 6 Micrographs of hydrate-bearing sediments with hydrate saturation of 0.24

saturation, the distribution of gas hydrates in sediments transforms from crystal particle to hydrate cement.

Experiment of hydrate dissociation

After all hydrate-bearing sediments were prepared, the relationship between acoustic velocity and hydrate saturation should be obtained. Then, experiment of hydrate dissociation can be conducted by closing valve 2 and opening other valves.

During hydrate dissociation experiment, drilling fluid was heated first in temperature control tank for ~1 h until its temperature reaches the required experimental temperature. Then, circulating pump was turned on, and its flow rate was stabilized as 2L/min. Two minutes later, temperature in cold storage and pore pressure of hydrate-bearing sediment in autoclave were adjusted to 15.25 degrees Celsius (initial reservoir temperature) and 15.50 MPa (initial reservoir pressure), respectively. Finally, the two-day experiment was started by adjusting the bottom-hole pressure to the experimental value through the mud pressure control pump. In experiment, the wave velocities were recorded once every 10 min by the ultrasonic measurement system. The received acoustic velocity was converted to hydrate saturation by Eqs. (2) in ultrasonic measurement system.

$$S_h = P_v(S_h) \tag{2}$$

where $P_v(S_h)$ is the function describing the relationship between P-wave velocity and hydrate saturation obtained in experiment.

Results and discussion

Relationship between hydrate saturation and P-wave velocity

As mentioned above, hydrate dissociation around wellbore during drilling operation was assessed through the distribution of hydrate saturation. Before hydrate dissociation experiment, the relationship between hydrate saturation and acoustic velocity (i.e., $P_v(S_h)$ in Eqs. (2)) needs to be explored first. To highlight the representativeness of experimental data, 8 of 40 transducers were randomly turned on every time the acoustic velocity measurement was conducted for hydrate-bearing sediment with specific hydrate saturation. The measurement results of acoustic velocity are given in Table 2. As observed in Table 2, for sediment with specific hydrate saturation, 8 velocity data present little difference.

However, statistical significance test is the premise for obtaining function $P_v(S_h)$. To this end, the statistical analysis was conducted with "one-way ANOVA" in IBM SPSS Statistics 25. The results of error analysis and significance analysis are shown in Table 3 and Table 4, respectively. Table 3 shows that the maximum standard error and maximum standard deviation are only 0.002645 and 0.007482, respectively. The errors may be caused by the slight lateral (i.e., radial and circumferential) difference in hydrate saturation in sediment during preparation of hydrate-bearing sediment. Additionally, as observed in Table 4, the significance P is 0.000, which is less than 0.050. Therefore, the effect of hydrate saturation on acoustic velocity

Table 2 Measurement results for hydrate-bearing sediment with specific hydrate saturation

Transducers No	Acoustic velocity of hydrate-bearing sediments with different S_h, km/s						
	$S_h=0$	$S_h=0.08$	$S_h=0.16$	$S_h=0.24$	$S_h=0.32$	$S_h=0.40$	$S_h=0.48$
1	1.397	1.433	1.541	1.787	2.065	2.418	2.853
2	1.393	1.438	1.536	1.783	2.062	2.407	2.846
3	1.391	1.429	1.539	1.786	2.057	2.426	2.848
4	1.402	1.431	1.538	1.791	2.069	2.415	2.842
5	1.395	1.435	1.543	1.788	2.062	2.410	2.840
6	1.389	1.436	1.542	1.784	2.071	2.421	2.845
7	1.401	1.435	1.544	1.776	2.063	2.418	2.838
8	1.406	1.432	1.540	1.793	2.067	2.416	2.861

Table 3 Error analysis results

Items	$S_h=0$	$S_h=0.08$	$S_h=0.16$	$S_h=0.24$	$S_h=0.32$	$S_h=0.40$	$S_h=0.48$
Average value, km/s	1.3968	1.4336	1.5404	1.7871	2.0645	2.4164	2.8466
Standard deviation	0.005874	0.002925	0.002669	0.003441	0.004472	0.005975	0.007482
Standard error	0.002077	0.001034	0.000944	0.001217	0.001581	0.002112	0.002645

Table 4 Significance test results (One way ANOVA)

	Sum of squares	df	Mean square	F	Significance, P
Between group	14.382	6	2.397	96,598.508	0.000
In group	0.001	48	0.000	-	-
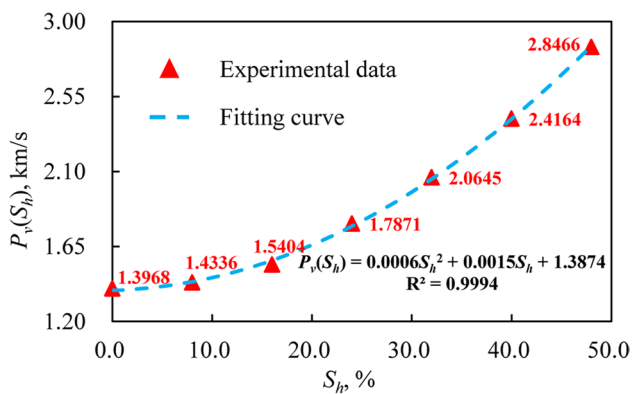
Fig. 7 Relationship between acoustic velocity $P_v(S_h)$ and hydrate saturation S_h

$$P_v(S_h) = 0.0006S_h^2 + 0.0015S_h + 1.3874 \ (R^2 = 0.9994) \quad (3)$$

Notably, for Eqs.(3), the correlation coefficient R^2 is 0.994, indicating that hydrate saturation can be determined by inversion of acoustic velocity obtained in hydrate dissociation experiments.

Evolution characteristics of hydrate dissociation around wellbore

Hydrate dissociation is an important factor causing wellbore instability while drilling in hydrate reservoir. Therefore, it is necessary to deeply explore the evolution characteristics of hydrate dissociation around wellbore during the drilling operation. Based on the experimental conditions (default case) in Table 5, Fig. 8 displays the distribution nephogram of hydrate saturation in sediment at different experimental moments. As observed in Fig. 8, hydrate saturation at the position with the same distance from borehole on any path is basically equal to each other at the same experimental moment. Therefore, the distribution of hydrate saturation in sediment during the experiment can be represented by that on any path. In this study, experiments are all based on the conditions shown in Table 5 if no specific statement is made.

Figure 9 demonstrates the distribution evolution of hydrate saturation along Path-1 around wellbore. Figure 9

of sediment is statistically significant (F = 96,598.507, P = 0.000 < 0.050).

Taking the average acoustic velocity as the standard, Fig. 7 displays the relationship between acoustic velocity and hydrate saturation. Figure 7 shows that acoustic velocity increases with hydrate saturation in the form of a nonlinear quadratic function. However, the specific quantification needs to be achieved through data fitting. After fitting operation in Excel, the relationship between acoustic velocity and hydrate saturation is expressed by Eqs. (3).

Table 5 Experimental conditions of default case

Experimental condition	Unit	Value
Hydrate saturation	-	0.24
Stabilizer concentration	wt%	0.30
Mud pressure	MPa	14.84
Mud temperature	K	296.40
Environment temperature	K	288.40
Reservoir pressure	MPa	14.55
Circulation flow rate	L/min	2.0
Total experimental time	h	48

shows that the dissociation of natural gas hydrates firstly occurs in area near borehole due to the disturbance of drilling fluid at the beginning of experiment. When the experiment goes on for 0.5 h, hydrate saturation at the borehole wall decreases to 0.172, and the width of the dissociation transition area is 0.52 times the borehole radius (expressed as $0.52r_b$). After that, caused by the continuous disturbance of drilling fluid, hydrate dissociation gradually occurs outward along the radial direction, and the dissociation transition area thereby widens. When the experiment has lasted for 1.0 h and 4.0 h, the width of the dissociation transition area reaches $1.13r_b$ and $2.96r_b$, respectively. However, natural gas hydrates at the borehole wall do not completely dissociate until 12.0 h after the experiment starts, which means that the completely dissociation area appears since this moment. Meanwhile, the width of the dissociation transition area is $5.91r_b$ when the experiment has lasted for 12.0 h. In addition, with the continuation of the experiment, hydrate dissociation continues to occur at locations further away from the borehole. When the experiment was over, the width of the completely dissociation area has reached $1.34r_b$, and the rest of the sediment is in the dissociation transition area.

In experiment, the dissociation rate of gas hydrates is not constant. The dissociation rate of gas hydrate along Path-1 (see Fig. 3a) for different experimental moments is as shown in Fig. 10. Notably, the dissociation rate of gas hydrates used herein is obtained by:

$$D_v = \frac{dS_h}{dt} \tag{4}$$

where dt is time interval and dS_h is the change of hydrate saturation in dt time interval.

As observed in Fig. 10, at the beginning of the experiment, gas hydrates in area near borehole dissociate fastest. The maximum dissociation rate is 0.0113 s^{-1} when the experiment goes on for 0.5 h, and the position where gas hydrates dissociate fastest is the borehole wall. As the experiment remains, the position where fastest hydrate

dissociation occurs gradually moves away from the borehole, and the maximum dissociation rate also dropped sharply. At the experimental moment of 12.0 h, the maximum dissociation rate is 0.0032 s^{-1}, which is only 28.32% of that when the experiment is carried out for 0.5 h. What is more, at the end of the experiment, positions with the maximum hydrate dissociation rate are about $4.25r_b$ away from the borehole wall, and the maximum hydrate dissociation rate has been only 0.0013 s^{-1}. Thereby, Fig. 10 shows that if the experiment continues after two days, hydrate dissociation rate at all positions will be lower. The mechanism why hydrate dissociation gradually weakens in experiment is shown in Fig. 11. As observed in Fig. 11, hydrate dissociation is an endothermic reaction, so hydrate dissociation will cause the decrease in reservoir temperature. Besides, dissociation products (mainly methane and water) of gas hydrates can also lead to the increase in local pore pressure. Both the decrease in reservoir temperature and the increase in pore pressure caused by hydrate dissociation will inhibit its further dissociation. Furthermore, the above changes of reservoir temperature and pore pressure caused by hydrate dissociation will also restrain the heat transfer to the position farther away from the borehole. Thereby, hydrate dissociation at the position farther away from borehole will also be suppressed at the subsequent experimental moments.

Comparison of the present experimental study with published simulation works

As mentioned in introduction, this study can provide basic experimental data for verification of some numerical simulation models that used for the investigation of hydrate dissociation around wellbore. Therefore, differences between results of the present experimental investigation and the previous simulations should be explored in detail. Comparison of the experimental results with those obtained by two numerical simulation models in published works has been made in this section, and the comparison results are demonstrated in Fig. 12.

As what we can see in Fig. 12, there are some differences between results of two numerical simulations and this experimental investigation. Among them, the most significant difference is the width of the dissociation transition area. In both numerical simulations in Fig. 12, the width of the dissociation transition area is significantly compressed and is relatively constant throughout the simulation. For the simulation based on the model given by Freij-Ayob et al. (2007), the width of the dissociation transition area is almost always maintained at about $1.15r_b$ during the whole simulation. Similarly, for the simulation based on the model given by Ning et al. (2013a, b), in the whole simulation, the width of the dissociation transition area is maintained at about

Fig. 8 Distribution nephogram of hydrate saturation in sediment at different experimental moments. (**a**) 0.5 h; (**b**) 2.0 h; (**c**) 12.0 h; (**d**) 24 h; (**e**) 48 h
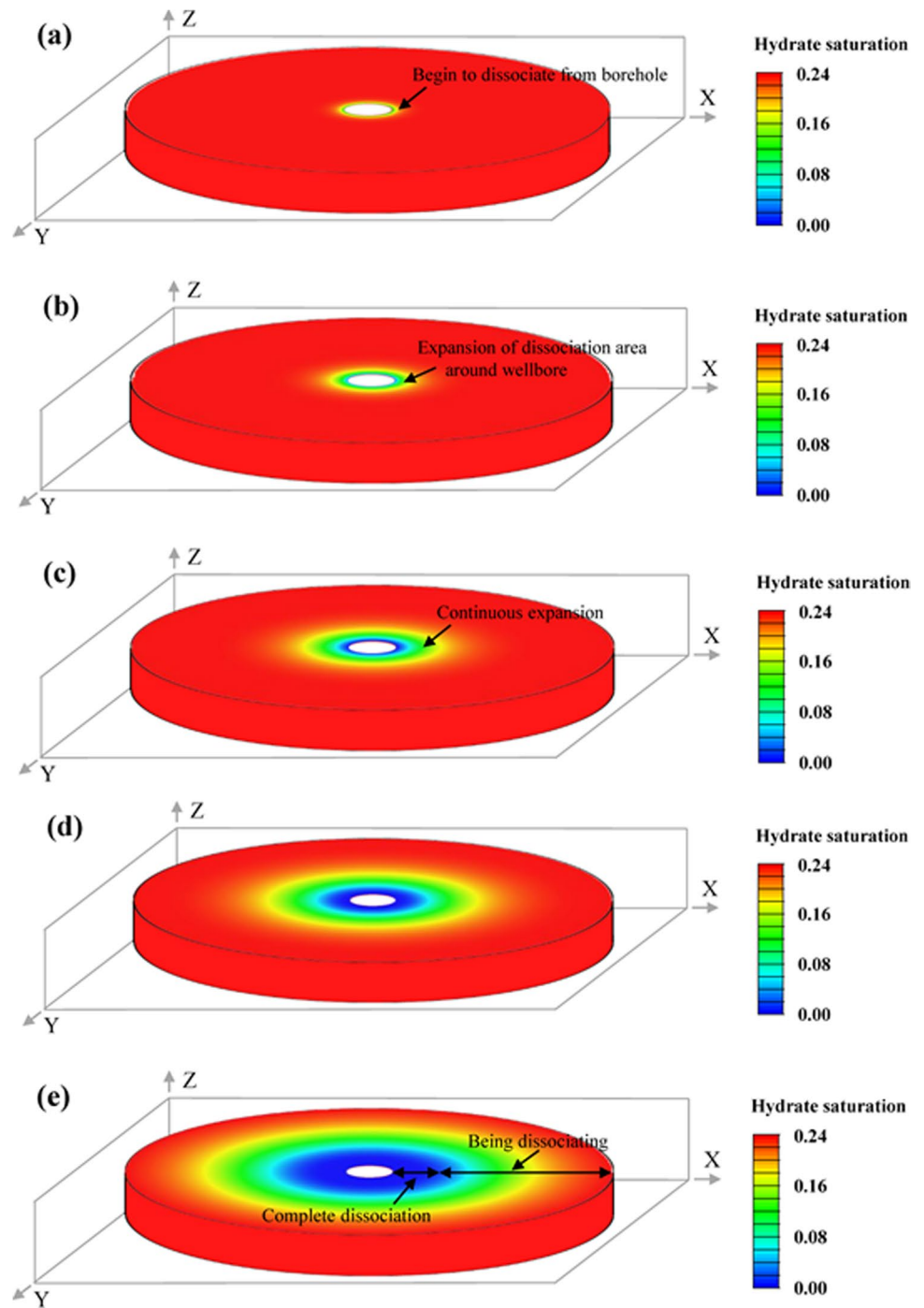
$1.31r_b$. However, the width of the dissociation transition area at any experimental moments is obviously wider than that in both numerical simulations. Moreover, the width of the dissociation transition area becomes wider and wider as the experiment continues. At 4.0 h, 12.0 h and 24.0 h, the width of the dissociation transition area in the present experiment is $3.36r_b$, $5.71r_b$ and $8.68r_b$. At 48.0 h, the position where gas hydrates begin to dissociate is no longer in sediment, so the width of the dissociation transition area at this experimental moment is not discussed. Yet, Fig. 12d shows that the width of the dissociation transition area is undoubtedly greater than $8.68r_b$ at the end of the experiment.

Figure 12 shows that the positions where gas hydrates start to dissociate are almost the same in two numerical simulations, as well as in the experiment. However, we have already known that the width of the dissociation transition area is obviously different from each other between the present experiment and previous numerical
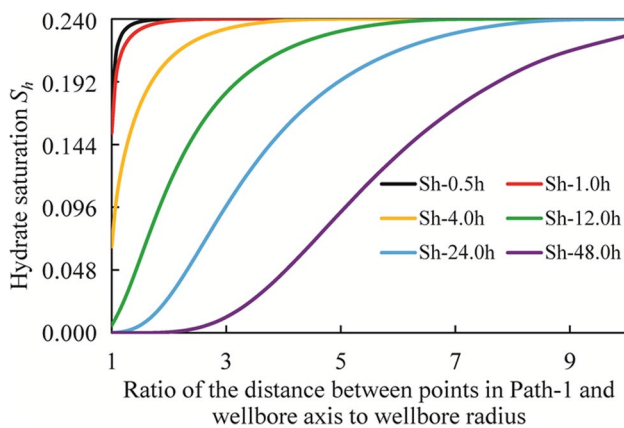
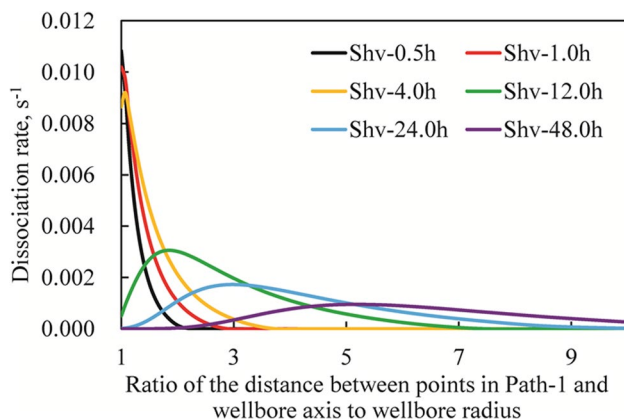**Fig. 9** Distribution of hydrate saturation along Path-1 at different experimental moments

Fig. 10 Dissociation rate of natural gas hydrate along Path-1 at different experimental moments

simulations. Thereby, the range of the completely dissociation area obtained by experiment is naturally different from that obtained by previous simulations. As previously mentioned, in experiment, gas hydrates at borehole wall do not completely dissociate until 12.0 h after the experiment starts, and the final range of the completely dissociation area is only $1.34r_b$. However, for both numerical simulations in Fig. 12, gas hydrates at the borehole wall have completely dissociated at the beginning of simulation. Moreover, as two simulations continue, the range of the completely dissociation area will gradually expand. For simulation based on a model developed by Freij-Ayob et al. (2007), the range of the completely dissociation area is $2.75r_b$, $4.15r_b$, $6.32r_b$ and $8.25r_b$, respectively, at 4.0 h, 12.0 h, 24 h and 48 h. Likewise, for simulation based on a model developed by Ning et al. (2013a, b), the range of the completely dissociation area is $2.14r_b$, $3.56r_b$, $5.63r_b$ and $7.65r_b$, respectively, at 4.0 h, 12.0 h, 24 h and 48 h.
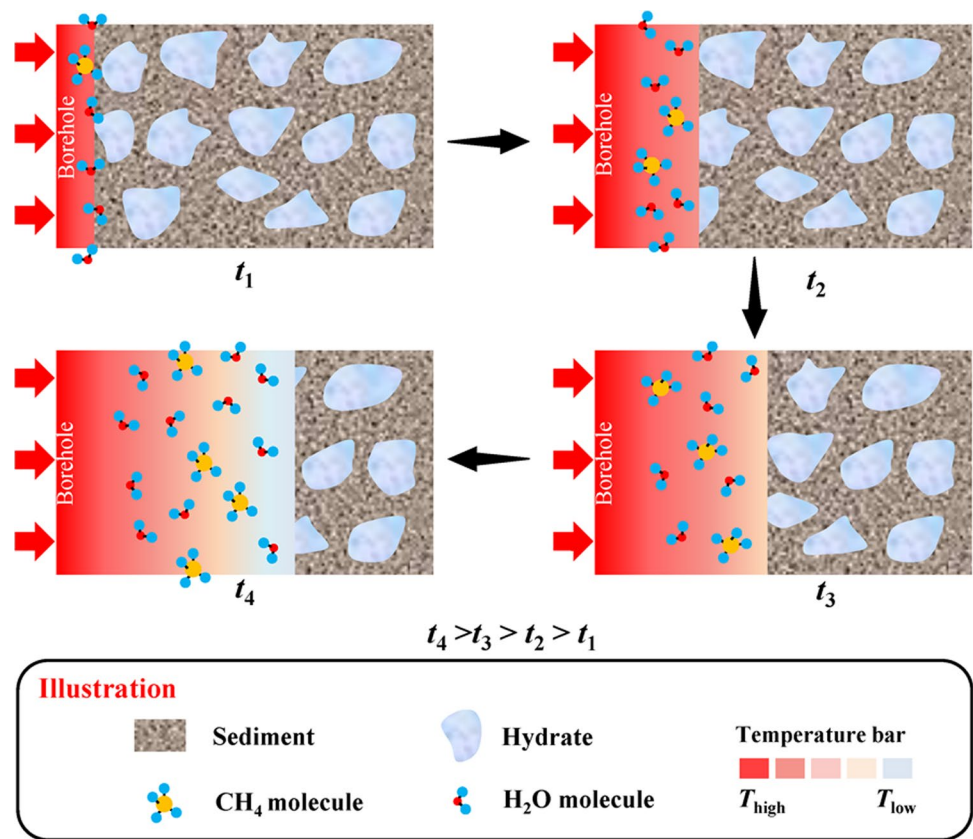
Actually, the difference between the experimental results and the simulation results is mainly attributed to the inappropriate understanding of the dissociation mode in numerical modeling. In numerical simulations, it is generally assumed that hydrate dissociation gradually advances outward from the borehole wall in the form of "thin piston," and the "thin piston" is exactly the dissociation transition area. Besides, it is also believed that natural gas hydrate in dissociation transition area can rapidly dissociate in numerical modeling, so that the dissociation transition area can move outward to the next position. Therefore, as observed in Fig. 12, the width of the dissociation transition area is basically unchanged throughout the simulation, and the completely dissociation area can appear rapidly and widen continuously. In fact, this is not exactly the case. In drilling operation, natural gas hydrates in the near-wellbore region dissociate outward in the form of a gradually widening dissociation transition area, not the form of "thin piston." Inaccurate simulation of hydrate dissociation affects the accuracy of borehole stability prediction. Thereby, in numerical modeling of hydrate dissociation around wellbore in the near-wellbore region, not only more conditions need to be considered, but also the dissociation mode needs to be further modified.

Hydrate dissociation for sediments with different hydrate saturation

Borehole stability can be influenced by hydrate saturation through affecting hydrate dissociation around wellbore. Therefore, investigations on hydrate dissociation in hydrate-bearing sediments with different hydrate saturations need to be conducted.

In this section, effect of hydrate saturation on hydrate dissociation in the near-wellbore region was investigated, and the experimental result is displayed in Fig. 13. As observed in Fig. 13, for all hydrate saturations studied herein, hydrates at any position of the sediment have begun to dissociate or have completely dissociated at the end of experiment. Figure 13 shows that the dissociation of natural gas hydrates in sediments weakens nonlinearly with the increase in the hydrate saturation. In the range of low hydrate saturation ($S_h \leq 0.24$), hydrate dissociation weakens so obviously with the increase in the hydrate saturation. If the range of the completely dissociation area is used to describe it, the final range of the completely dissociation area narrows rapidly within the range of low hydrate saturation as the hydrate saturation increases. When hydrate saturation is only 0.08, gas hydrates in sediments dissociate rapidly in experiment, and the final range of the completely dissociation area reaches $4.28r_b$. However, when hydrate saturation has increases to 0.24, the final range of the completely dissociation area has decreased to $1.34r_b$, which is $2.94r_b$ narrower than that

Fig. 11 Schematic of temperature distribution around wellbore during hydrate dissociation in near-wellbore region

$t_4 > t_3 > t_2 > t_1$

Illustration

Sediment | Hydrate | Temperature bar

CH_4 molecule | H_2O molecule | T_{high} T_{low}

when the hydrate saturation is 0.08. Notably, when hydrate saturation exceeds 0.24, the phenomenon that hydrate dissociation weakens as hydrate saturation increases has become less obvious. When hydrate saturation increases from 0.24 to 0.48, the final range of the completely dissociation area only decreases from $1.34r_b$ to $0.53r_b$, and the decline is only $0.81r_b$. We can boldly infer that if hydrate saturation continues to increase, the final width of the completely dissociation area will be narrower than $0.53r_b$.

Figure 14 schematically illustrates the reason why hydrate dissociation weakens with the increase in the hydrate saturation in drilling operation. We all know that the heat required for completely dissociating the specific amount of gas hydrates is constant. As observed in Fig. 14, for all cases, heat Q is assumed to be transferred into the cube infinitesimal element with side length dr in the same time interval dt. If hydrate saturation is high (see Fig. 14a, assuming S_{hhigh}), the heat Q provided by drilling fluid can only make gas hydrates in sediment with the width of dr' in infinitesimal element completely dissociate. However, if hydrate saturation is low (see Fig. 14b, assuming S_{hlow}), the heat Q can make gas hydrates in sediment with the width of dr'' in infinitesimal element completely dissociate. The relationship between dr'' and dr' can be expressed by Eqs. (5):

$$dr^{\varepsilon} = dr' \frac{S_{hhigh}}{S_{hlow}} \tag{5}$$

Since S_{hhigh} is assumed to be higher than S_{hlow}, dr'' is always wider than dr'. And, the greater the difference between S_{hhigh} and S_{hlow}, the wider dr'' is than dr'.

Effect of stabilizer concentration on hydrate dissociation

As an environmentally friendly additive for drilling fluid, soybean lecithin is a by-product in the process of refining soybean oil and will not have a serious impact on the marine environment. So, soybean lecithin is a hydrate stabilizer worthy of recommendation. In the present study, the effect of soybean lecithin concentration on hydrate dissociation has also been investigated. Figure 15 displays the final width of the completely dissociation area and dissociation transition area when the stabilizer concentration in the drilling fluid is different. As shown in Fig. 15, the width of the completely dissociation area decreases as the stabilizer concentration increases until it reaches 0. The width of the completely dissociation area is $6.42r_b$ when there is no soybean lecithin in drilling fluid. However, when the stabilizer concentration reaches 0.60wt%, both the width of the completely

Fig. 12 Distribution of hydrate saturation along a radial path around ▶
wellbore that obtained by experiment and two simulation methods in
different references, respectively. (**a**) 4.0 h; (**b**) 12.0 h; (**c**) 24.0 h; (**d**)
48.0 h

dissociation area and the width of the dissociation transi-
tion area are 0. In other words, when the concentration of
soybean lecithin is higher than 0.60wt%, the dissociation of
natural gas hydrates in the near-wellbore region around well-
bore can be completely prevented during drilling operation.
All these indicate that the addition of soybean lecithin in
drilling fluid will have a better inhibitory effect on the disso-
ciation of gas hydrates around wellbore in drilling operation.

Previous studies have shown that soybean lecithin does
not affect the stability of hydrate by changing the thermody-
namic equilibrium conditions (Chen et al. 2007). In fact, just
as displayed in Fig. 16, soybean lecithin inhibits hydrate dis-
sociation by forming the mesh membrane on hydrate surface
to limit mass transfer. Transfer of water and methane mol-
ecules from the hydrate surface to the fluid in pores is free
if there is no soybean lecithin in drilling fluid (see Fig. 16a).
That is to say, the mass transfer resistance can almost be
ignored when the concentration of soybean lecithin is 0.
With the increase in concentration of soybean lecithin, the
mass transfer resistance gradually increases due to the for-
mation of mesh membrane on the hydrate surface. When
its concentration is not very high, adjacent soybean lecithin
molecules form local mesh membrane on hydrate surface
(see Fig. 16b). In this case, some of the water and methane
molecules produced by hydrate dissociation are blocked on
the hydrate surface by the mesh membrane, and further dis-
sociation of gas hydrates is inhibited to some extent. How-
ever, if the concentration of soybean lecithin is high enough,
the mesh membrane formed by soybean lecithin can com-
pletely cover the hydrate surface (see Fig. 16c). Transfer of
almost all water and methane molecules from the hydrate
surface to the fluid in pores is blocked, and no hydrate disso-
ciation can continue to occur in the subsequent experiment.

Prevention of uncontrollable hydrate dissociation and accompanying methane leakage

As mentioned above, methane leakage caused by hydrate
dissociation in drilling operation poses the threat to the
marine environment and the marine organisms, as well as
the drilling safety. To prevent the marine environmental
issues such as borehole collapse or methane leakage while
drilling in hydrate reservoir, reducing hydrate dissociation
around wellbore is the key. Adding environmental-friendly
hydrate stabilizer (such as soybean lecithin) to drilling fluid
is an environmental and effective measure. Nevertheless, the
stabilizer concentration in drilling fluid needs to be designed
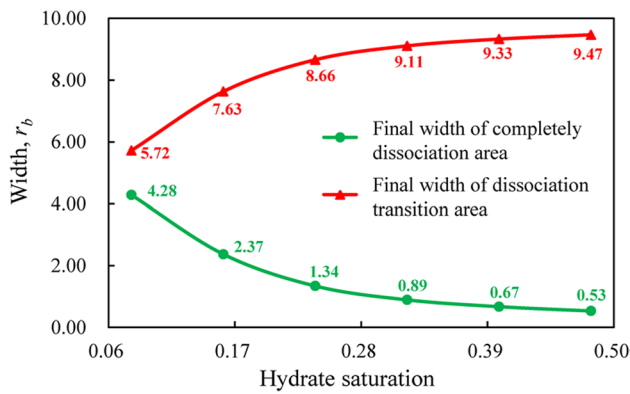in advance according to acceptable hydrate dissociation or
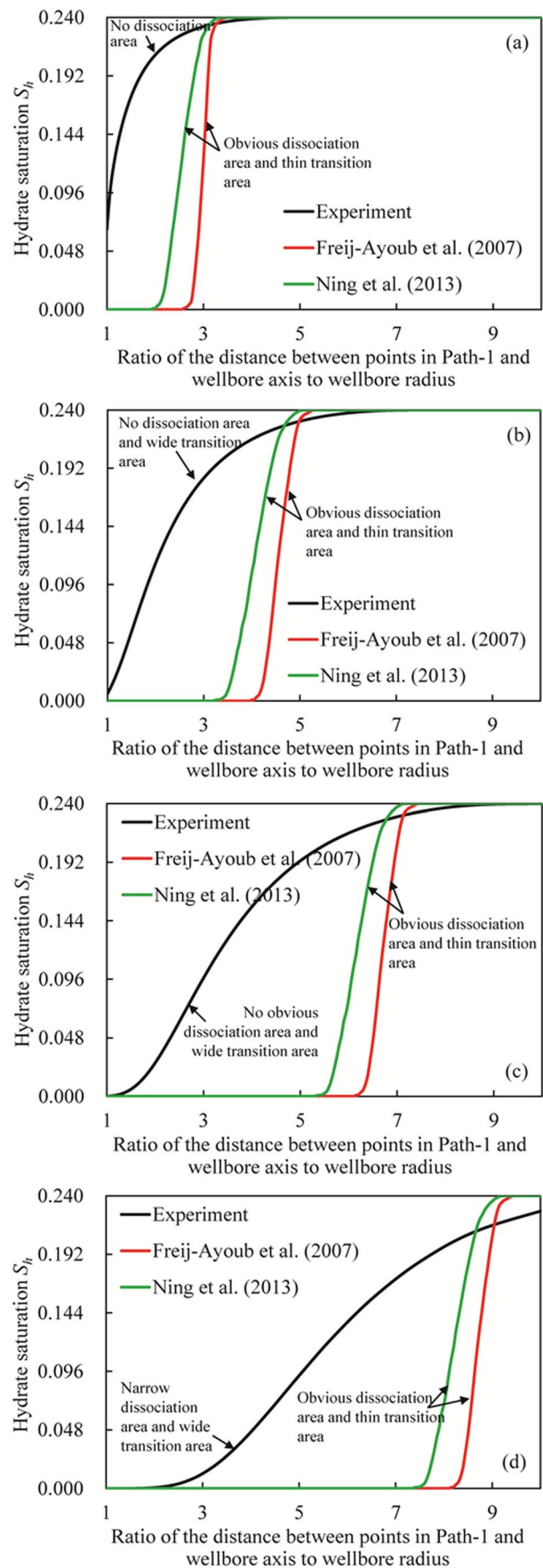
Fig. 13 Effect of hydrate saturation on hydrate dissociation around wellbore during drilling operation

methane leakage. In terms of the experimental conditions herein, if it is required that hydrate dissociation and methane leakage cannot occur in drilling operation, concentration of soybean lecithin needs to be higher than 0.60wt%. However, it is unrealistic not to allow hydrate dissociation and methane leakage during drilling operation. According to Fig. 15, if hydrates in sediment with a width of $0.5r_b$ around wellbore is allowed to completely dissociate, the concentration of soybean lecithin needs to be at least 0.39wt%. Similarly, through Fig. 15, we can determine the lower limit of soybean lecithin concentration corresponding to any acceptable

width of completely dissociation area required by marine environmental protection.

Conclusions

In this study, an experimental apparatus used for determination of hydrate saturation by ultrasonic measurement was designed and assembled, and the influence of various factors on hydrate dissociation around wellbore during drilling in hydrate reservoir was also investigated. In order to reduce drilling risk and marine environmental pollution, engineering recommendations to prevent uncontrollable hydrate dissociation and methane leakage are given according to the experimental results. Method for determination of hydrate saturation in hydrate-bearing sediment was obtained by fitting the relationship between hydrate saturation and acoustic velocity. Through error analysis, it is concluded that this method has high accuracy and can be used extensively to determine hydrate saturation in hydrate-bearing sediments. Comparison between the experimental results of hydrate dissociation with the simulation results obtained by the numerical model given in previous numerical studies reveals obvious difference between them. This concludes that the previous numerical model needs to be properly modified in terms of dissociation mode with reference to the experimental results

Fig. 14 Schematic diagram of the influence mechanism of hydrate saturation on hydrate dissociation in sediments around wellbore

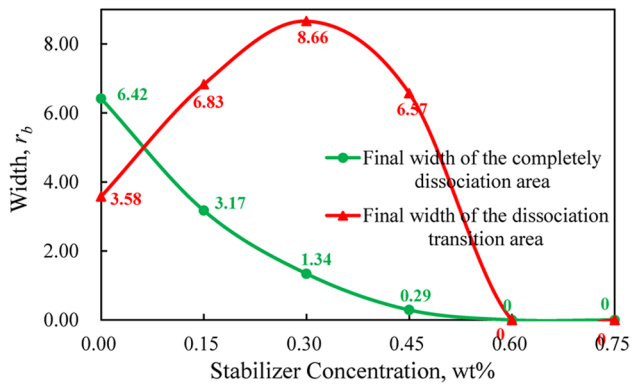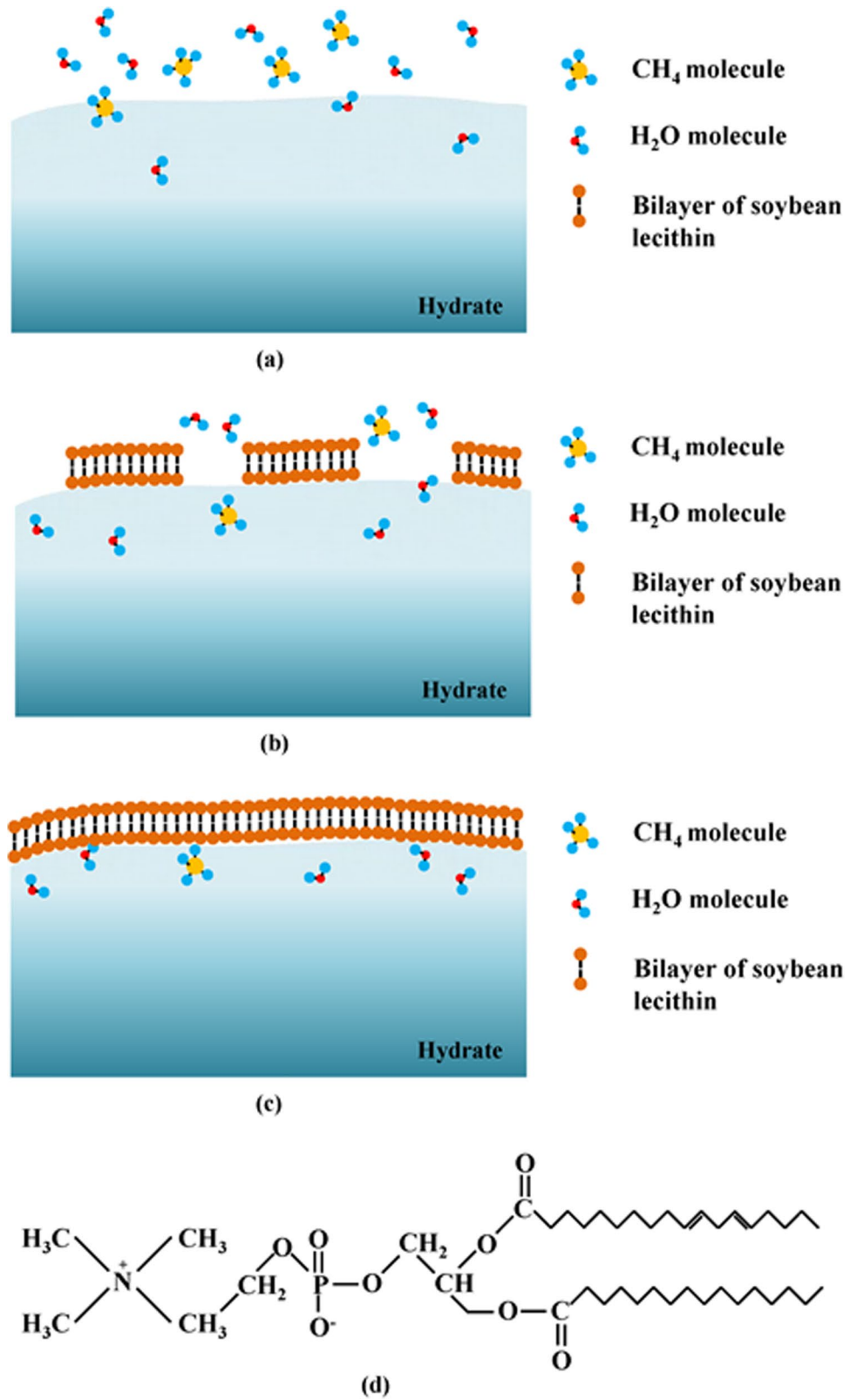
(a) High saturation
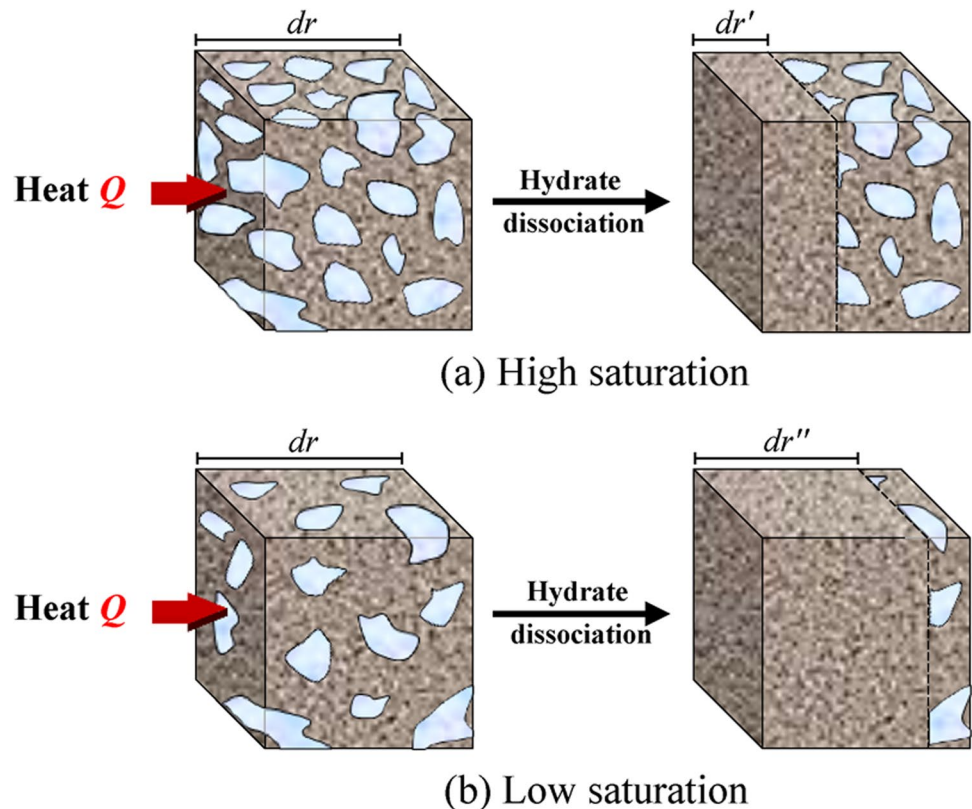
(b) Low saturation

Fig. 15 Effect of stabilizer concentration on hydrate dissociation around wellbore during drilling operation

when it was used in the future. In addition, although the increase in the hydrate saturation and soybean lecithin concentration can both weaken hydrate dissociation in experiment, the latter has a better effect. Depending on Fig. 15, if no hydrate dissociation was acceptable in both of drilling safety and environmental protection, concentration of soybean lecithin in drilling fluid should be at least 0.60wt%. Overall, no matter what the requirement for hydrate dissociation is, concentration of soybean lecithin in drilling fluid can be adjusted in real time according to Fig. 15. Investigation in the present work not only helps to reduce the risk of drilling operation, but also provides technical support for reducing greenhouse gas emissions and protecting the marine environment.

Fig. 16 Stabilization mechanism of soybean lecithin on gas hydrate. (**a**) no soybean lecithin in drilling fluid; (**b**) low concentration of soybean lecithin in drilling fluid; (**c**) high concentration of soybean lecithin in drilling fluid; (**d**) molecular structure of lecithin

References

Ashena R, Elmgerbi A, Rasouli V, Ghalambor A, Rabiei M, Bahrami A (2020) Severe wellbore instability in a complex lithology formation necessitating casing while drilling and continuous circulation system. J Pet Explor Prod Te 10(4):1511–1532. https://doi.org/10.1007/s13202-020-00834-3

Chen W, Patil SL, Kamath VA, Chukwu GA (2007) Effect of lecithin on methane hydrate formation. Huagong Xuebao (Chin. Ed.) 58(11):2895–2900

Cheng W, Lu C, Ning F, Jia M (2021) A coupled thermal-hydraulic-mechanical model for the kinetic dissociation of methane hydrate in a depressurizing well. J Pet Sci Eng 207:109021. https://doi.org/10.1016/j.petrol.2021.109021

Freij-Ayoub R, Tan C, Clennell B, Tohidi B, Yang J (2007) A wellbore stability model for hydrate bearing sediments. J Pet Sci Eng 57(1–2):209–220. https://doi.org/10.1016/j.petrol.2005.10.011

Gambelli AM (2021) Analyses on CH_4 and CO_2 hydrate formation to define the optimal pressure for CO_2 injection to maximize the replacement efficiency into natural gas hydrate in presence of a silica-based natural porous medium, via depressurization techniques. Chem Eng Process 167:108512. https://doi.org/10.1016/j.cep.2021.108512

Gao Y, Chen Y, Wang Z, Chen L, Zhao X, Sun B (2019) Experimental study on heat transfer in hydrate-bearing reservoirs during drilling processes. Ocean Eng 183:262–269. https://doi.org/10.1016/j.oceaneng.2019.04.092

Golmohammadi S, Nakhaee A (2015) A cylindrical model for hydrate dissociation near wellbore during drilling operations. J Nat Gas Sci Eng 27(part 3):1641–1648. https://doi.org/10.1016/j.jngse.2015.10.032

Huang T, Li X, Zhang Y, Wang Y, Chen Z (2020) Experimental study of the drilling process in hydrate-bearing sediments under different circulation rates of drilling fluid. J Pet Sci Eng 189:107001. https://doi.org/10.1016/j.petrol.2020.107001

Joseph J, Dangayach S, Singh D, Kumar P, Dewri S, Tandi C, Singh J (2017) Investigation on excess gas method for synthesis of methane gas hydrates. J Nat Gas Sci Eng 42:203–215. https://doi.org/10.1016/j.jngse.2017.02.043

Li Q, Liu L, Yu B, Guo L, Shi S, Miao L (2021a) Borehole enlargement rate as a measure of borehole instability in hydrate reservoir and its relationship with drilling mud density. J Pet Explor Prod Te 11(3):1185–1198. https://doi.org/10.1007/s13202-021-01097-2

Li Y, Liu C, Liao H, Lin D, Bu Q, Liu Z (2021b) Mechanical properties of the clayey-silty sediment-natural gas hydrate mixed system. Nat Gas Ind B 8(2):154–162. https://doi.org/10.1016/j.ngib.2020.08.002

Liu W, Liu R, Zhang M, Liu Z, Lang C, Li Y (2021) Rheological properties of hydrate slurry formed from mudflows in south China Sea. Energy Fuels 35(13):10575–10583. https://doi.org/10.1021/acs.energyfuels.1c01294

Li Y, Cheng Y, Yan C, Song L, Ren X (2020) Mechanical study on the wellbore stability of horizontal wells in natural gas hydrate reservoirs. J Nat Gas Sci Eng 79:103359. https://doi.org/10.1016/j.jngse.2020.103359

Misyura SY (2020) Developing the environmentally friendly technologies of combustion of gas hydrates. Reducing harmful emissions during combustion. Environ Pollut 265(Part A):114871. https://doi.org/10.1016/j.envpol.2020.114871

Ning F, Zhang K, Wu N, Zhang L, Li G, Jiang G, Yu Y, Liu L, Qin Y (2013a) Invasion of drilling mud into gas-hydrate-bearing sediments. Part I: effect of drilling mud properties. Geophys J Int 193(3):1370–1384. https://doi.org/10.1093/gji/ggt015

Ning F, Wu N, Yu Y, Zhang K, Jiang G, Zhang L, Sun J, Zheng M (2013b) Invasion of drilling mud into gas-hydrate-bearing sediments. Part II: Effects of geophysical properties of sediments. Geophys J Int 193(3):1385–1398. https://doi.org/10.1093/gji/ggt016

Sahu C, Kumar R, Sangwai J (2021) A comprehensive review on well completion operations and artificial lift techniques for methane gas production from natural gas hydrate reservoirs. Energy Fuels 35(15):11740–11760. https://doi.org/10.1021/acs.energyfuels.1c01437

Salehabadi M (2009) Hydrates in sediments: their role in wellbore/casing integrity and CO_2 sequestration. Ph.D. Thesis; Heriot-Watt University.

Sell K, Saenger E, Falenty A, Chaouachi M, Haberthür D, Enzmann F, Kuhs W, Kersten M (2016) On the path to the digital rock physics of gas hydrate-bearing sediments – processing of in situ synchrotron-tomography data. Solid Earth 7:1243–1258. https://doi.org/10.5194/se-7-1243-2016

Sloan ED (2003) Fundamental principles and applications of natural gas hydrates. Nature 426(6964):353–359. https://doi.org/10.1038/nature02135

Song B, Cheng Y, Yan C, Lyu Y, Wei J, Ding J (2019) Li Y (2019) Seafloor subsidence response and submarine slope stability evaluation in response to hydrate dissociation. J Nat Gas Sci Eng 65:197–211. https://doi.org/10.1016/j.jngse.2019.02.009

Wang L, Jiang G, Zhang X (2021a) Modeling and Molecular Simulation of Natural Gas Hydrate Stabilizers. Eur J Remote Sens 54(sup2):21–32. https://doi.org/10.1080/22797254.2020.1738901

Wang Y, Lang X, Fan S, Wang S, Yu C, Li G (2021b) Review on enhanced technology of natural gas hydrate recovery by carbon dioxide replacement. Energy Fuels 35(5):3659–3674. https://doi.org/10.1021/acs.energyfuels.0c04138

Yan C, Cheng Y, Li M, Han Z, Zhang H, Li Q, Teng F, Ding J (2017) Mechanical experiments and constitutive model of natural gas hydrate reservoirs. Int J Hydrogen Energy 42(31):19810–19818. https://doi.org/10.1016/j.ijhydene.2017.06.135

Yan C, Yang L, Cheng Y, Wang W, Song B, Deng F, Feng Y (2018) Sand production evaluation during gas production from natural gas hydrates. J Nat Gas Sci Eng 57:77–88. https://doi.org/10.1016/j.jngse.2018.07.006

Yan C, Ren X, Cheng Y, Song B, Li Y, Tian W (2020) Geomechanical issues in the exploitation of natural gas hydrate. Gondwana Res 81:403–422. https://doi.org/10.1016/j.gr.2019.11.014

Yang E, Fang Y, Liu Y, Li Z, Wu J (2020) Research and application of microfoam selective water plugging agent in shallow low-temperature reservoirs. J Petrol Sci Eng 193:107354. https://doi.org/10.1016/j.petrol.2020.107354

Yang L, Wang J, Yang Y, Sun G (2021) Numerical analysis of soil deformation and collapse due to hydrate decomposition. ACS Omega 6:5335–5347. https://doi.org/10.1021/acsomega.0c05463

Yao Y, Wei M, Kang W (2021) A review of wettability alteration using surfactants in carbonate reservoirs. Adv Colloid Interfac 294:102477. https://doi.org/10.1016/j.cis.2021.102477

Yao Y, Wei M, Bai B (2022) Descriptive statistical analysis of experimental data for wettability alteration with surfactants in carbonate reservoirs. Fuel 310:122110. https://doi.org/10.1016/j.fuel.2021.122110

Ye J, Qin X, Qiu H, Xie W, Lu H, Lu C, Zhou J, Liu J, Yang T, Cao J, Sa R (2018) Data report: molecular and isotopic compositions of the extracted gas from China's first offshore natural gas hydrate production test in south China Sea. Energies 11(10):2793. https://doi.org/10.3390/en11102793

Ye J, Qin X, Xie W, Lu H, Ma B, Qiu H, Liang J, Lu J, Kuang Z, Lu C, Liang Q, Wei S, Yu Y, Liu C, Li B, Shen K, Shi H, Lu Q, Li J, Kou B, Song G, Li B, Zhang H, Lu H, Ma C, Dong Y, Bian H (2020) The second natural gas hydrate production test in the south China Sea. China Geology 3(2):197–209. https://doi.org/10.31035/cg2020043

Yu L, Xu Y, Gong Z, Huang F, Zhang L, Ren S (2018) Experimental study and numerical modeling of methane hydrate dissociation and gas invasion during drilling through hydrate bearing formations. J Pet Sci Eng 168:507–520. https://doi.org/10.1016/j.petrol.2018.05.046

Zhang J, Sun Q, Wang Z, Wang J, Sun X, Liu Z, Sun B, Sun J (2021) Prediction of hydrate formation and plugging in the trial production pipes of offshore natural gas hydrates. J Clean Prod 316(20):128262. https://doi.org/10.1016/j.jclepro.2021.128262

Zhao X, Qiu Z, Wang M, Xu J, Huang W (2019a) Experimental investigation of the effect of drilling fluid on wellbore stability in shallow unconsolidated formations in deep water. J Pet Sci Eng 175:595–603. https://doi.org/10.1016/j.petrol.2018.12.067

Zhao X, Qiu Z, Zhao C, Xu J, Zhang Y (2019b) Inhibitory effect of water-based drilling fluid on methane hydrate dissociation. Chem Eng Sci 199:113–122. https://doi.org/10.1016/j.ces.2018.12.057

Zhong H, Yang T, Yin H, Lu J, Fu C (2020) Role of Alkali Type in Chemical Loss and ASP-Flooding Enhanced Oil Recovery in Sandstone Formations. SPE Reserv Eval Eng 23(2):431–445. https://doi.org/10.2118/191545-PA

Zhu Y, Wang P, Pang S, Zhang S, Xiao R (2021) A review of the resource and test production of natural gas hydrates in China. Energy Fuels 35(11):9137–9150. https://doi.org/10.1021/acs.energyfuels.1c00485